J Electroceram (2012) 28:209–213
DOI 10.1007/s10832-012-9682-y

Correlation between crystal structure and properties of ultra-high dielectric constant ceramics x $SrCO_3$-Bi_2O_3-Ag(Nb,Ta)O_3

Peng Yin · Li Lingxia · Cao Lifeng · Liao Qingwei

Received: 8 August 2011 / Accepted: 14 November 2011 / Published online: 4 April 2012

Abstract The correlation between crystal structure and properties of x wt% $SrCO_3$-4.5 wt.%Bi_2O_3-Ag($Nb_{0.8}Ta_{0.2}$)O_3 (x $SrCO_3$-Bi_2O_3-ANT) (x=0.5~3.0) dielectric ceramics was investigated. The permittivity was significantly influenced by the redshift of three typical vibration modes of A_{1g}(Ag), F_{2g}(Nb/Ta) and A_{1g}(O). The dielectric loss was optimized by the restraint of the second phase $AgNbO_3$, and a minimum value was obtained when x=2.0. Changes of c/a value, which indicate the degree of lattice distortion, reflected the temperature coefficient of relative permittivity (τ_ε) was highly correlated with the crystal structure and a near zero τ_ε value was achieved with 2.0 wt.% Sr concentration. The Bi_2O_3-doped ANT ceramics containing 2.0 wt.% $SrCO_3$ sintered at 1150°C showed excellent dielectric properties: an ε_r value of 841, a tan δ value of 0.00119 and a near zero (−23.7 ppm/°C) τ_ε value.

Keywords Dielectric ceramics · Ag(Nb,Ta)O_3 · Raman spectra · Crystal structure

1 Introduction

Consumers' demands for multi-functional pocket or credit-card-sized devices are motivating the development of microwave wireless-communication and information systems. Such level of miniaturization can only be realized by dielectric materials with ultra-high permittivity. The perovoskite-type Ag(Nb,Ta)O_3 ceramic possesses excellent properties, i.e. low dielectric loss ($<18\times10^{-4}$) and extraordinary high permittivity (>430), which makes it a highly potential candidate for wireless-communication, microelectric technologies, and miniaturization of microwave components [1–3].

In recent years, investigations of different ion substitutions on the physical properties of Ag(Nb,Ta)O_3 ceramics were undertaken and considerable progresses have been obtained. Guo et al. [4] investigated substitution Sb_2O_5 for ($Nb_{0.8}Ta_{0.2}$)$_2O_5$ in the Ag($Nb_{0.8}Ta_{0.2}$)O_3 ceramics, and Ag($Nb_{0.8}Ta_{0.2}$)$_{1-x}Sb_xO_3$ solid solutions were prepared with permittivity of 825, dielectric loss of 0.0023, and τ_ε of −38.52 ppm/°C. Ag($Nb_{0.8}Ta_{0.2}$)O_3 ceramics with 4.5 wt.% CaF_2 addition possessed a ε_r of 1028, a tan δ of 8.6×10^{-4} and a τ_ε value of −50 ppm/°C (at 1 MHz) [5]. Sonia Duguey et al. [6] showed that Ag(Nb_xTa_{1-x})O_3 solid solutions with a given amount of copper substitution present a permittivity of 415 and a $Q{\cdot}f$ value of 610 GHz. Guo et al. [7] also reported that proper amount of Bi_2O_3 substitution in the Ag(Nb_xTa_{1-x})O_3 ceramics can effectively decrease the tan δ and improve the ε_r and τ_ε value.

According to previous works, the Bi_2O_3-doped ANT ceramics could be a potential candidate for microwave devices. However, a comprehensive performance (higher ε_r, lower tan δ and near zero τ_ε value) still need to be optimized for practical use, and further works on the synergistic effect of two or more different additives on the ANT ceramics have not been satisfactory. Since a few works have found that the $Q{\cdot}f$ value could be improved by partial Sr substitution for Ba, and the τ_f decreased with the

P. Yin · L. Lingxia (✉) · C. Lifeng · L. Qingwei
School of Electronic and Information Engineering,
Tianjin University,
Tianjin 300072, China
e-mail: lilingxia@tju.edu.cn

P. Yin
e-mail: pengy0613@gmail.com

increasing content of Sr substitution for Ba in $A_5B_4O_{15}$ and $A_6B_5O_{18}$ (A=Ba, Sr) systems [8, 9]. R. Rawal et al. [10] have found that the measured τ_f value (of $Sr_3LaNb_3O_{12}$ ceramic) is −9 ppm/°C which is much closer to zero ppm/°C compared with that of $Ba_3LaNb_3O_{12}$ (−100 ppm/°C). In this sense, partial Sr substitution for A-site ions in ANT system might lower the dielectric loss and τ_ε value.

In this work, $SrCO_3$ was selected as a further additive for the Bi_2O_3-doped ANT ceramics (with a fixed Bi_2O_3 content of 4.5 wt.%). The synergistic effect of Sr^{2+} and Bi^{3+} on the dielectric properties of ANT was investigated. And the correlation between crystal structure and dielectric properties was also discussed.

2 Experimental procedure

Reagent grade Nb_2O_5, Ta_2O_5, Ag_2O, Bi_2O_3 and $SrCO_3$ were used as starting materials to synthesize $xSrCO_3$-4.5 wt.%Bi_2O_3-$Ag(Nb_{0.8}Ta_{0.2})O_3$ ($xSrCO_3$-Bi_2O_3-ANT) ceramics. Firstly, $(Nb_{0.8}Ta_{0.2})_2O_5$ precursor was synthesized by preheating Nb_2O_5 and Ta_2O_5 mixture at the temperature of 1200°C for 6 h. Then, Ag_2O was added according to the formula of $Ag(Nb_{1-x}Ta_x)O_3$ and mixed using distilled water and zirconia milling media. The mixed powders were calcined at 1050°C for 6 h to form ANT. Bi_2O_3 and $SrCO_3$ with appropriate stoichiometric proportion were used as additives and then reground together with ANT. The milled powders were granulated, and then the granules were pressed into disks with 10 mm in diameter and 1–1.5 mm in thickness. These samples were conventionally sintered at 1100–1160°C in air for 4 h, with the heating rate of 5°C/min.

Microstructures of the sintered samples were examined using Scanning Electron Microscopy (Phillips XL30). Crystal structures of the samples were studied by an X-ray diffract meter (Rigaku 2038) using Cu Kα radiation. The dielectric capacitance and dielectric loss were measured at 1 MHz with a capacitance meter (Agilent HP4278A). Raman measurements for the sintered samples were carried out at room temperature (Bruker FS100). The excitation source was the 1064 nm line with 100 mw Raman laser power. The recorded Raman spectra exhibited approximately 2 cm^{-1} resolution. τ_ε was tested by C-T parameter measuring equipment comprised of an oven (GZ-ESPEC) and a HM 27002 Capacitor C-T Meter Model. The τ_ε value was defined as the following equation:

$$\tau_\varepsilon = \frac{\varepsilon_{85} - \varepsilon_{25}}{\varepsilon_{25}} \times 10^6 = \frac{C_{85} - C_{25}}{C_{25}} \times 10^6 (ppm/^\circ C)$$

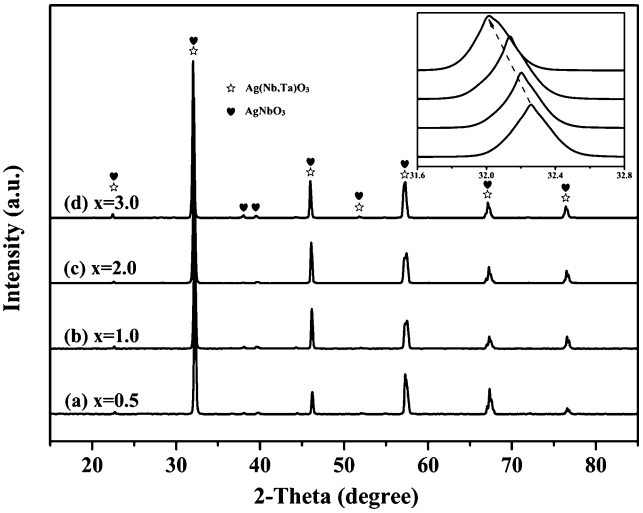

Fig. 1 XRD patterns of x $SrCO_3$-Bi_2O_3-ANT (x=0.5, 1.0, 2.0, 3.0) ceramics

where the C_{85} and C_{25} are the capacitance of a sample tested at 85°C and 25°C respectively and ε_{85} and ε_{25} are the corresponding relative permittivity calculated from the capacitances.

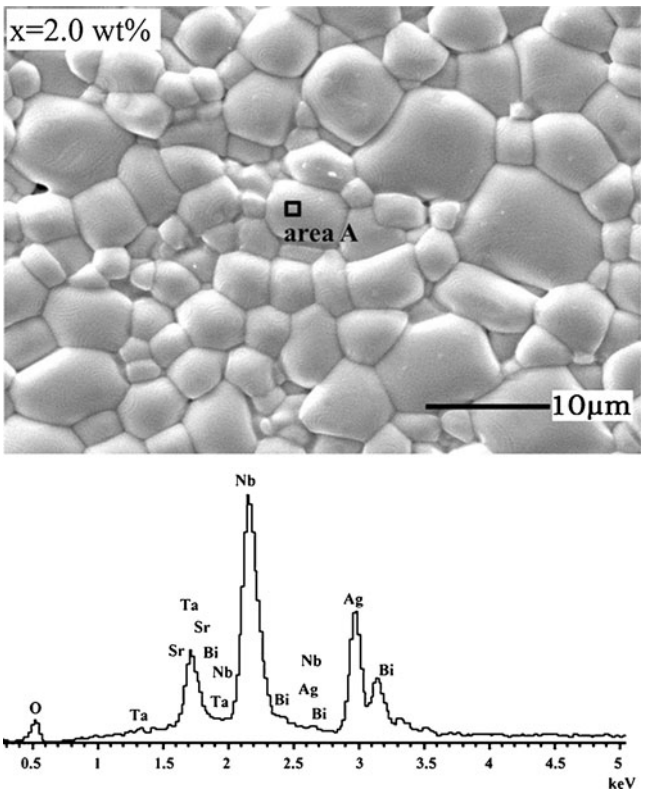

Fig. 2 SEM micrographs and EDS analysis of 2.0 wt.%$SrCO_3$-Bi_2O_3-ANT ceramics

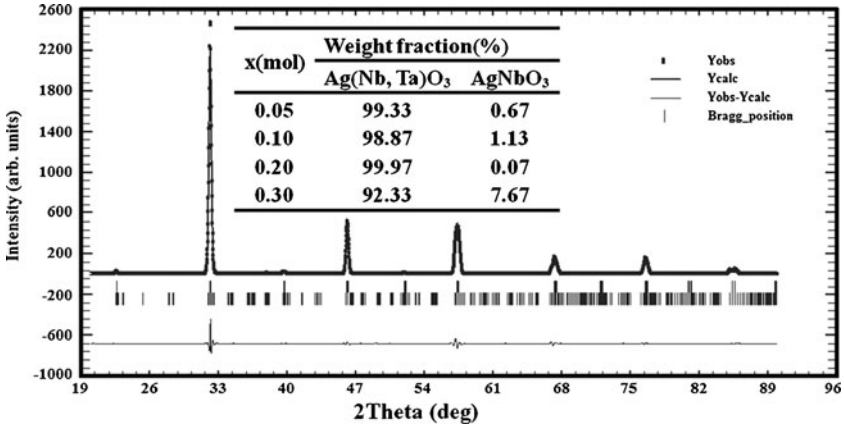

Fig. 3 The typical pattern of multiple refinement of 2.0 $SrCO_3$-Bi_2O_3-ANT ceramics

3 Results and discussion

3.1 Structure analysis

3.1.1 X-ray diffraction analysis

Figure 1 shows the XRD characterization of various amounts of Sr^{2+} doped 4.5 wt.% Bi_2O_3-ANT samples, and the $AgNb_{0.5}Ta_{0.5}O_3$ (JCPDS #53-0347) and $AgNbO_3$ (JCPDS #52-0405) phases were obtained. No additional Sr^{2+} or Bi^{3+}-contained phase could be detected by XRD. So it was inferred that a solid solution was formed with the Sr^{2+} addition, which could be further interpreted by the SEM and EDAX results illustrated in Fig. 2. The SEM micrograph and EDAX spectrum indicated that Sr^{2+} and Bi^{3+} ions entered the lattice of the host crystal. The relative weight fractions of crystalline phases shown in Fig. 2 were calculated directly from scale factors which obtained by the quantitative phase analysis using the Rietveld refinement. All parameters of interest including background, zero-point, scale factors for all phases, half-width, unit-cell parameters, atomic positional coordinates, temperature factors were refined step-by-step for avoiding correlations. The $AgNb_{0.5}Ta_{0.5}O_3$ (ICSD #88050) reported by M. Valant et al. [11] and $AgNbO_3$ (ICSD #280359) reported by J. Farbry et al. [12] were adopted as the starting model. Figure 3 shows a typical pattern plot after refinement of all parameters of interest. The calculated pattern is overlaid on the measured pattern and the differences between two profiles are plotted along the bottom. Part of refinement results were shown in Table 1.

3.1.2 Raman spectrum analysis

Typical Raman spectra of the non-doped $Ag(Nb_{0.8}Ta_{0.2})O_3$ ceramics (spectrum I), 4.5 wt.% Bi_2O_3 doped (spectrum II) and the sample with further 2.0 wt.% $SrCO_3$ (spectrum III) are illustrated in Fig. 4, Table 2 presents the locations and FHWM of the Raman bands of ANT system. For $Ag(Nb_{0.8}Ta_{0.2})O_3$ systems, the vibrations could be classified as internal modes of $(Nb,Ta)_2O_5$ octahedron and lattice translations involving motion of cations [13]. The lines near 104 cm^{-1} are due to A_{1g}(Ag), which could be assigned as motion of Ag^+. Bands due to niobium ions and tantalum ions occur at 212~251 cm^{-1} (F_{2g}(Nb/Ta)), while the modes associated with oxygen ions occur at 567 cm^{-1}(E_g(O)) and the weak lines near 800 cm^{-1}(A_{1g}(O)) [5].

Obviously, the A_{1g}(Ag) mode slightly shifts to a lower frequency, indicating the Ag-O bonds energy decreases with Bi^{3+} and Sr^{2+} concentration. Furthermore, an overlap

Table 1 Crystallographic data obtained from a Rietveld refinement for x $SrCO_3$-Bi_2O_3-ANT ceramics

	x	Lattice parameters (Å)			Vol. (Å^3)	c/a	S ($\times10^{-5}$)
		a	b	c			
$AgNb_{0.5}Ta_{0.5}O_3$	0.5	3.9354	3.9373	3.9339	60.9037	0.9996	3.4847
	1.0	3.9323	3.9316	3.9305	60.773	0.9994	3.3234
	2.0	3.9312	3.8984	3.9235	60.2816	0.9980	3.5345
	3.0	3.9375	3.8984	3.9444	61.1407	1.0017	3.1264
$AgNbO_3$	0.5	5.5563	5.5999	15.6571	487.1565	2.8179	0.0021
	1.0	5.5453	5.5887	15.6866	486.1385	2.8288	0.0034
	2.0	5.5468	5.5917	15.6662	485.8850	2.8243	0.0002
	3.0	5.5527	5.5939	15.6535	486.1842	2.8190	0.0232

x=0.50, Rp=6.35%, Rwp=9.85%, GOF=0.2056; *x*=1.0, Rp=9.14%, Rwp=14.7%, GOF=0.5029; *x*=2.0, Rp=7.17%, Rwp=11.9%, GOF=0.3359; *x*=3.0, Rp=6.58%, Rwp=11.3%, GOF=0.2932

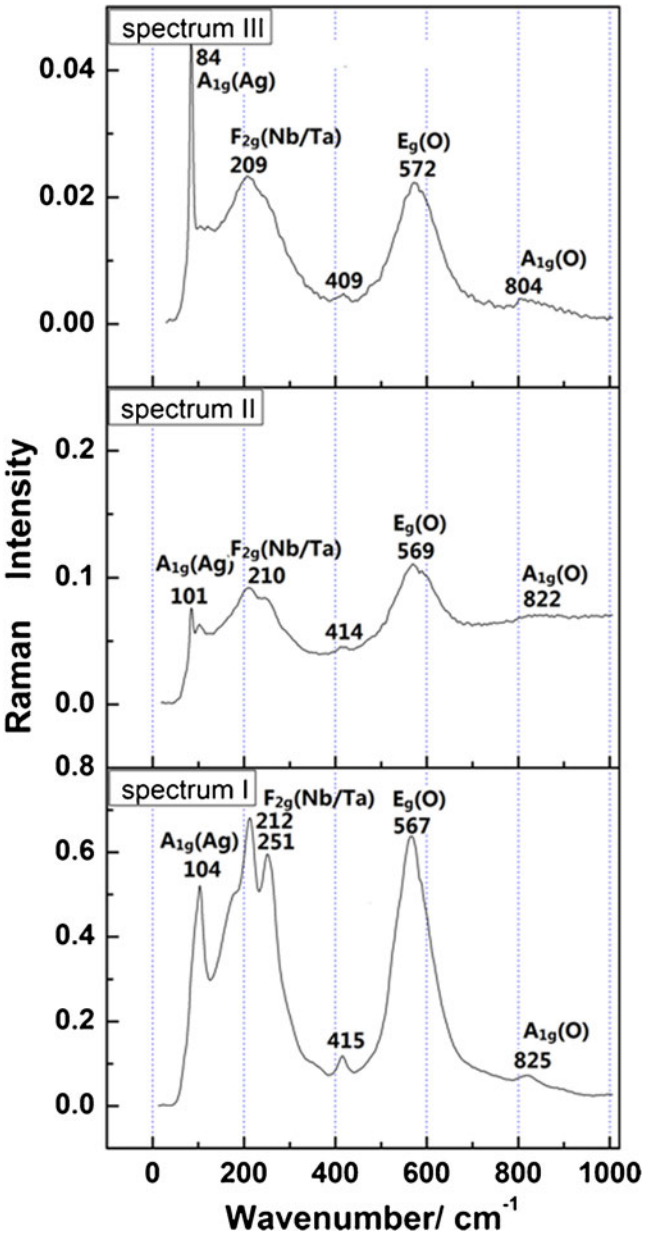

Fig. 4 Raman spectra for ANT (spectrum I), 4.5 wt.%Bi_2O_3-ANT (spectrum II) and 2.0 wt.%$SrCO_3$-Bi_2O_3- ANT (spectrum III) ceramics

Table 2 Raman fitting parameters for ANT system

Bands	ANT	Bi_2O_3-ANT	2.0 $SrCO_3$-Bi_2O_3-ANT
1	104(12.5)	101(12.1)	84(10.1)
2	212(23)	211(36)	205(35)
3	254(28)	244(28)	243(20)
4	415(25)	414(31)	409(15)
5	565(34)	563(71)	567(56)
6	568(13)	569(71)	572(56)
7	825(36)	822(65)	804(11)

Position and full width at half-maximum (in parentheses) are in cm^{-1}

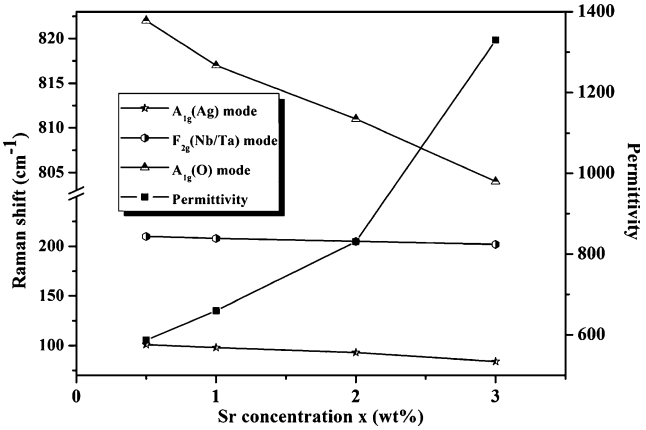

Fig. 5 Correlation of the A_{1g}(Ag), F_{2g}(Nb/Ta) and A_{1g}(O) modes of Raman shift with the permittivity for the x $SrCO_3$-Bi_2O_3-ANT ceramics

of the F_{2g}(Nb/Ta) mode occurred. In the above two vibration modes, the A_{1g}(Ag) mode was extremely sensitive to the Sr^{2+} concentration, indicating a large variation was induced in the Ag-O dodecahedron. So it could be concluded that the addition of Sr deteriorates the ordering in the ANT ceramics due to the Sr^{2+}, Bi^{3+} and Ag^{+} ions being able to easily rearrange their positions in the A-site.

The oxygen atoms' vibration along Nb-O-Ta direction and the vibration frequency of the mode is mainly affected by the strength of Nb-O and Ta-O bonds. The redshift of corresponding A_{1g}(O) modes indicates that Nb-O and Ta-O bonds become weak with increasing $SrCO_3$ content.

3.2 Dielectric properties

The characteristics of Raman resonance peak are closely related to the microwave dielectric properties of materials [14]. In Fig. 5, the Raman shift of A_{1g}(Ag), F_{2g}(Nb/Ta) and A_{1g}(O) modes were plotted versus the Sr concentration x for x$SrCO_3$-Bi_2O_3-ANT, as well as the correlation between

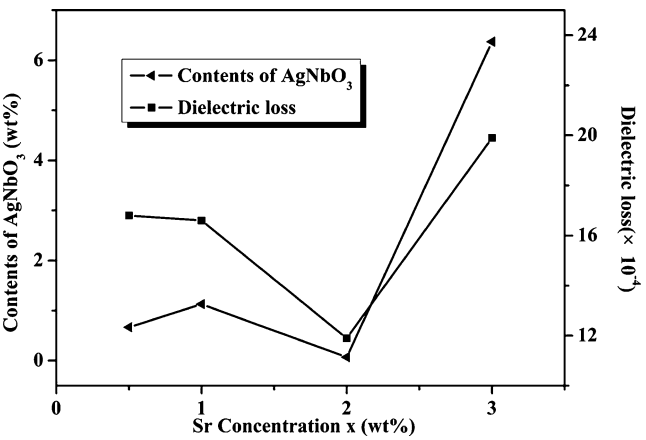

Fig. 6 Correlation of $AgNbO_3$ phase content with dielectric loss for the x $SrCO_3$-Bi_2O_3-ANT ceramics

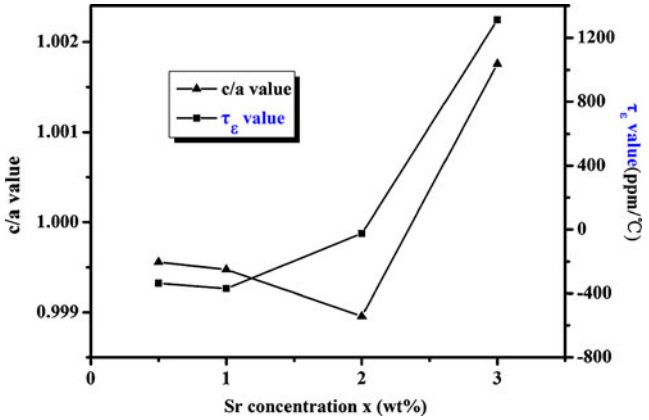

Fig. 7 Dependence of the τ_ε value of x $SrCO_3$-Bi_2O_3-ANT ceramics on the c/a value calculated from XRD refinement

Raman shift and the permittivity. As could be seen, the permittivity increases sharply as the Sr^{2+} concentration while the three modes plotted shows totally inverse trend. Combining with the previous XRD results, it was concluded that the addition of Bi^{3+} and Sr^{2+} deteriorates the ordering of A-site ions and $(Nb,Ta)_2O_5$ octahedron in the ANT ceramics, which could also be confirmed by the redshift of the three modes. In this case, the bonding forces between cations and oxygen atoms became weaker, which would cause the results that the $xSrCO_3$-Bi_2O_3-ANT permittivity increased along with x.

Many factors are believed to affect the losses of dielectric ceramics, which could be divided into intrinsic loss and extrinsic loss [15]. The intrinsic loss is caused by anharmonic phonon decay process in the pure crystal lattice while the extrinsic loss is caused by crystal defects, grain boundaries, second phases, and pores [16]. In this work, the dielectric loss is mainly influenced by the second phase of $AgNbO_3$, as shown in Fig. 6. The tendency of the dielectric loss varied with x was familiar with that of the content of the second phase. When x=2.0, the lowest dielectric loss value was obtained with the minimum content of $AgNbO_3$.

It's well known that c/a value is a typical characteristic of the degree of lattice distortion in perovskite structure [17]. The calculated c/a value of the previous system, illustrated in Table 1 and Fig. 7, demonstrated the x=2.0 samples possess a minimum distortion, and shows a near zero τ_ε value (−23.7 ppm/°C). In addition, Colla et al. [18] also suggested that the addition of larger A-site cations in a tilted structure make the τ_ε increase, which have quite similar trend with τ_ε depending on x value shown in Fig. 5.

4 Conclusions

X-ray tests showed that all samples studied consist of $Ag(Nb,Ta)O_3$ dominant perovskite phase with a minor $AgNbO_3$ phase. The Raman displacement of the vibration peak of $A_{1g}(Ag)$, $F_g(Nb/Ta)$ and $A_{1g}(O)$ modes indicated that the permittivity was significantly modified due to the vibration motion of A-site ions and the distortion of the crystal structure, which could be characterized by the redshift of Raman shift. The dielectric loss was significantly influenced by the presence of $AgNbO_3$; the comparison showed that a minimum dielectric loss was achieved due to the lowest content of the second phase. Temperature coefficient of relative permittivity was determined by the c/a value, the τ_ε value was adjusted to −23.7 ppm/°C when the c/a reached a minimum, 0.9980.

Acknowledgements This work was supported by Program for New Century Excellent Talents in University (NCET) and 863 Program (2007AA03Z423) and China Postdoctoral Science Foundation.

References

1. M. Valant, D. Suvorov, C. Hoffmann, H. Sommariva, J. Eur. Ceram. Soc. **21**, 2647 (2001)
2. M. Valant, D. Suvorov, J. Am. Ceram. Soc. **82**, 88 (1999)
3. H. Kim, T. Shrout, C. Randall, M. Lanagan, J. Am. Ceram. Soc. **85**, 2738 (2002)
4. X.Y. Guo, N. Zhu, J. Am. Ceram. Soc. **90**, 2467 (2007)
5. L.F. Cao, L.X. Li, P. Zhang, H.T. Wu, Rare. Met. **29**, 50 (2010)
6. S. Duguey, R. Lebourgeois, C. Grattepain, J. Heintz, J. Ganne, J. Eur. Ceram. Soc. **27**, 1171 (2007)
7. X.Y. Guo, M. Xiao, X.W. Wu, J. Chin. Ceram. Soc. **34**, 5 (2006)
8. I.N. Jawahar, P. Mohanan, M.T. Sebastian, Mater. Lett. **57**, 4043 (2003)
9. I.N. Jawahar, M.T. Sebastian, P. Mohanan, Mater. Sci. Eng. B. **106**, 207 (2004)
10. R. Rawal, A. Feteira, N.C. Hyatt, D.C. Sinclair, K. Sarma, N.M. Alford, J. Am. Ceram. Soc. **89**, 332 (2006)
11. M. Valant, D. Suvorov, J. Am. Ceram. Soc. **82**, 81 (1999)
12. J. Farbry, Z. Zikmund, A. Kania, V. Petricek. Acta. Crystallogr. C. **56**, 916 (2000)
13. S.D. Ross, J. Phys. C: Solid-State Phys. **3**, 1785 (1970)
14. H.-F. Cheng, Chia-Ta Chia, H.-L. Liu, Mei-Yu Chen, Y.-T. Tzeng, I-Nan Lin, J. Eur. Ceram. Soc. **27**, 2893 (2007)
15. W.S. Kim, T.H. Hong, E.S. Kim, K.H. Yoon, Jpn. J. Appl. Phys. **37**, 5367 (1998)
16. H. Tamura, Am. Ceram. Soc. Bull. **73**, 92 (1994)
17. K. Kageyama, J. Am. Ceram. Soc. **75**, 1767 (1992)
18. E.L. Colla, I.M. Reaney, N. Setter, J. Appl. Phys. **74**, 3414 (1993)